Journal of Operation and Automation in Power Engineering
Vol. 7, No. 1, May 2019, Pages: 49-57
http://joape.uma.ac.ir

High Gain Multi-Input DC-DC Converter with Combined Phase-Shift/PWM Modulation for Stand-Alone Applications

*P. khademi Astaneh, J.Javidan *, Kh.Valipour, A. Akbarimajd*

Department of Electrical Engineering, University of Mohaghegh Ardabili, Ardabil, Iran.

Abstract- *The objective of this paper is to introduce a new multi-input converter for a hybrid supply system containing photovoltaic, fuel cell, and battery for medium power applications. In this converter, the current ripple of fuel cell is removed, due to the utilization of a coupled inductor. Since, a combination of the magnetizing and the leakage inductors of two boosting transformers are used, a soft switching condition exists for semiconductors. To improve the reliability of the system, three switch-legs are used which results in distributed power transfer and increases the system redundancy from the reliability point of view. The steady state model and control system are discussed for the proposed converter. At the high voltage side of converter, two transformers are connected in series to achieve high voltage gain. An experimental prototype has been designed and examined in the laboratory to evaluate the proposed converter performance.*

Keyword: DC-DC converter, Multi-input converter, Soft switching, Hybrid power supply.

NOMENCLATURE

D_1	Duty cycle of the switch M_2.
D_2	Duty cycle of the switch M_6.
D_{o1}, D_{o2}	Output diodes.
L_{PV}	Inductor of PV boost cell.
L_b	Inductor of battery boost cell.
L_{FC}	Inductor of FC boost cell.
$M_1 - M_6$	The switches of the converter.
n_1, n_2	Transformers' secondary to primary turn ratios.

1. INTRODUCTION

Emerging green energy resources has given a new perspective to the world of science and industry. Increasing the air pollution and the global warming as well as reducing fossil fuel resources, have leaded the humanity to use the green energies, such as wind energy, photovoltaic, and etc. Using power electronic has been essentially applicable for utilizing these types of energy resources [1]–[5]. Reliability is one obvious issue of such resources.This problem can be resolved using energy storage units and other energy resources besides the main energy resource such as photovoltaic and wind energy [6]–[8]. This system can consist one unique converter having several ports and every energy resources and load are connected to this converter. The mentioned unique converter is called multi-input or multi-port converter [9], [10]. Utilizing such converters has the advantages of increasing system efficiency and reliability and improving system dynamic due to using the central controller.Many converters were proposed in the literature to manage power between multiple sources. Refs. [11], [12] discuss multi-port converters with time sharing strategy to control the power. In these converters, complex control strategy is required which is the result of changing the switching pattern in various power transfer situations. In Ref. [13] a family of three port converters are introduced by integrating conventional buck, boost, and buck boost converters. Although a very nice idea is behind the proposed converters, but the converters have some drawbacks such as low voltage gain, hard switching operation, and EMI issue. In Ref. [14] an isolated double input DC-DC converter is proposed by using an alternative pulsating source . Thanks to the utilization of isolating transformer, high voltage gain can be achieved in the aforementioned converter. However, the soft switching have not been achieved for all of the switches. Moreover, the number of switches are high but the voltage gain only depends on the transformer turn ratio.

Received: 04 March. 2018
Revised: 27 Aug. 2018
Accepted: 23 Sep. 2018
∗Corresponding author:
E-mail: javidan.javad@gmail.com (J. Javidan)
Digital object identifier: 10.22098/joape.2019.4515.1357
Research Paper

Ref. [15] introduces four port DC-DC converter with soft switching and time sharing power management strategy. The proposed structure contains pulsating voltages which are switched on the primary side of a flyback transformer. The main disadvantages of such structure are low voltage gain due to voltage-source operation of input ports and high input current ripple which can reduce the lifespan of fuel cells and reduce the efficiency of photovoltaic modules. In Ref. [16] a four port converter was proposed based on transformer isolation. But, the aforementioned converters suffers from low voltage gain and complex power management strategy due to time sharing method. Achieving high voltage gain, soft switching, and high efficiency capability are the most requirements in the converters for renewable energies. Also, single mode control strategy for power management in various demands, such as charging and discharging mode of battery, result in simplification for implementation.

This paper proposes a high voltage gain multi-input converter which uses soft switching technique, to apply in hybrid supply system for photovoltaic, fuel cell, and battery. Regarding low voltage level of energy resources and due to existence of the fuel cell in the system, the proposed converter is designed, so that the proper voltage gain can be reached. Furthermore, the current ripple drawn by fuel cell, is removed by using the coupled inductor in the fuel cell resource. Consequently it improves the fuel cell behavior. The soft switching of switches is occurred by magnetizing energy and the transformers leakage inductances. The diodes would have no reverse recovery current if an appropriate leakage inductance is used. The proposed converter is shown in Fig.1. There are two voltage levels in this converter. The low voltage level is in the primary side and the high voltage level is in the secondary side of the transformers. The primary side of the converter contains three switch legs connected to three boost cells. Energy transmission takes place in the low voltage DC link between three energy resources and no energy passes through the transformers for energy transmission between sources. It improves the converter efficiency in the battery charging mode. So the proposed converter has the following characteristics:

- Zero voltage soft switching for the switches
- Zero current soft switching for the diodes
- High efficiency
- Energy transmission to the load through two routes which increases the reliability of the system.
- The energy distribution between three legs and two transformers improves the heat transfer capability.
- High voltage gain

Section 2 discusses the proposed converter structure. Section 3 presents the operating principles and the design consideration. In this section, behavior of the converter will be examined over one cycle, first. Then the foregoing analysis will be used to evaluate the voltage gain of the converter. In the following, the power transmitted to each ports of the converter is determined mathematically. Eventually, the efficiency calculation is discussed which is accomplished for various loads and operating modes. Section 4 provides the results of an experimental prototype of the proposed converter. Final section includes a brief discussion about manifest characteristics of the proposed converter.

2. THE PROPOSED CONVERTER

The schematic of the proposed multi-input DC-DC converter is shown in Fig. 1. The converter consists of three power sources dedicated for PV, FC, and battery, two boost cells to increase the low input voltages of power sources to higher intermediate DC link V_C, a phase shift full bridge cell, two voltage transformers and a voltage double. The input voltage V_{PV} and V_{FC} are the voltages produced by PV array and Fuel cell, respectively. The third port is allotted to battery for energy storage purpose.

To express the functionality of each part of the converter, it should be noted that three boost cells are used. The boost cells are $M_1 - M_2 - L_{PV} - C$, $M_1 - M_2 - L_b - C$, and $M_5 - M_6 - L_{FC} - C - C_1$. The third one is a ripple free boost cell which is used for fuel cell. In addition to that, two phase-shift bridges are used in which the outputs are connected in series. The phase-shift cells are $M_1 - M_2 - M_3 - M_4 - T_1$ and $M_3 - M_4 - M_5 - M_6 - T_2$. The output side of T_1 and T_2 are connected in series to achieve higher voltage gain. In addition the secondary side of the transformers T_1 and T_2 are connected to a voltage doubler including D_{o1}, D_{o2}, C_{o1}, and C_{o2}. These result in a high voltage gain structure.

To manage the power between three input sources and the output port, following strategy is used: Pulse Width Modulation (PWM) switching method is used for power management between V_{PV} and V_b. M_2 and M_1 are on for $D_1 T_s$ and $(1 - D_1)T_s$, respectively. Hence, D_1 in this switch leg controls power between V_{PV} and V_b, which will be explained further. Switch leg 3 is controlled by PWM to control the power delivery from V_{FC}, and finally, switch leg 2 is switched by a half of switching period to control the power transmitted to output port, by creating phase shifted voltage on the transformers.

To analyze operation modes of the converter, power sources are modeled by an ideal voltage source series with an internal resistance. A coupled inductor L_{FC} is modelled as an ideal transformer with magnetizing inductor L_m parallel with input winding and a leakage inductor L_k series with output winding. It will be shown that a coupled inductor helps the FC to have a ripple free input current.

The fuel cell is connected to the DC link, similarly. The coupled inductor used through the fuel cell to its switch leg, is only considered from the circuit point of view, where the coupled inductor removes current ripple by referring DC ripple, associated to the fuel cell current, to its secondary. Therefore, the elements C - M_6 - M_5 - L_{FC} will form a boost converter, which is responsible for energy management between the fuel cell and the DC link. Power is transmitted to the output load through two boosting transformers. The transformers T_1 and T_2 are placed between the legs 1 and 2 and the legs 3 and 4, respectively. Switches of the leg 2 operate with $D = 0.5$. The voltage across the transformers are changed by phase shifting of the legs 1 and 3, respect to the leg 2. This strategy can be regarded to control the power transmitted to the output.

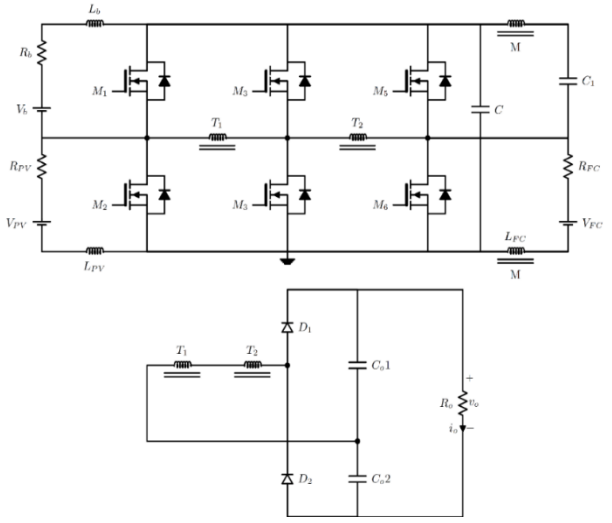

Fig. 1. Proposed multi-input DC-DC converter

3. DESIGN CONSIDERATIONS

Having the knowledge of what have been mentioned in prior section would be helpful to investigate the behavior of the converter over a cycle. Then the converter voltage gain will be derived in a simple form and applied in order to explain the management power procedure in the converter. Thereupon, the converter gain is obtained by calculating the elements losses, to evaluate the proposed system performance.

3.1. Principles of the proposed converter operation

In this section, the converter behavior over a cycle is to be paid attention. As stated in the former section, the proposed converter enjoys a set including three boost cells, in the primary side. Two boosting transformers are used in the converter, to isolate the low-voltage side from the high-voltage side. Both transformers inputs are connected to the three switch legs and their outputs are in series. Using two transformers and three switches cause power transmitted into the converter to be feasible through two ways. Besides, generated heat is distributed among more elements and transmitted much easier. Following assumptions are applied to analyze the converter:

- All of the switches and diodes are considered ideal.
- Inductor and capacitor noise resistive are neglected.
- The coupled inductor is modeled as an ideal transformer including a parallel L_m in the input and a L_k in the output.
- Leakage inductance of the transformer is negligible.
- Input sources (photovoltaic, fuel cell, and battery), are modeled as an ideal source connected in series with a resistor.

Moreover, the parameters D_1 and D_2 are defined as duty cycles of the switch 1 and switch 2, respectively. n is a parameter to represent the ratio of the number of turns in secondary to the number of turns in primary for the coupled inductor. n_1 and n_2 have the same definitions for the transformers 1 and 2, respectively. It should be noted that, the switches of the leg 2 are switching by a duty cycle equal to 50 percent. Fig. 2 illustrates the proposed converter in details, considering the foregoing assumptions and key wave forms of the converter are demonstrated in Fig. 3.

Interval 1 $[t_0, t_1]$: in the beginning of this interval, the switch S_3 is turned off. In this interval the capacitor of the drain source of the switch S_4 is discharged by the energy existing in the magnetizing inductor of the two transformers connected to this leg and the capacitor of the switch S_3 is charged. At the same time, the parallel reverse diode of the switch S_4 is turned on after discharging its capacitor. Hence the switch S_4 is ready to turn on in soft switching conditions.

Interval 2 $[t_1, t_2]$: at the starting point of this interval, the switch S_4 is turned on under ZVS conditions. Before this time interval, the switches 1 and 5 were ON. Therefore, in this interval, the voltage across the inputs of both transformers equals v_c . This voltage makes the magnetizing current of the two transformers, be increased from the most negative value. The secondary side of the boosting transformers has the same voltage relative to the

turn ratio. So, the diode D_{o1}, which was OFF in the beginning of this interval, starts to conduct by a positive voltage being across that. The following expression can be written for the equivalent leakage inductance of the two transformers in this interval.

$$L_k \frac{di_k}{dt} = 2(n_1 + n_2)v_C - v_{o1} \quad (1)$$

Moreover, as the switches M_1 and M_5 are ON, the inductors L_{m1} and L_{PV} discharge. But, the inductor L_b is charged. Accordingly the mathematical model of input side of the converter can be written as follows:

$$L_{PV} \frac{di_{PV}}{dt} = V_{PV} - V_C \quad (2)$$

$$L_b \frac{di_b}{dt} = V_b \quad (3)$$

$$L_m \frac{di_m}{dt} = V_{FC} - V_C \quad (4)$$

$$L_{K1} \frac{di_{k1}}{dt} = n(V_{FC} - V_C) - V_{C1} \quad (5)$$

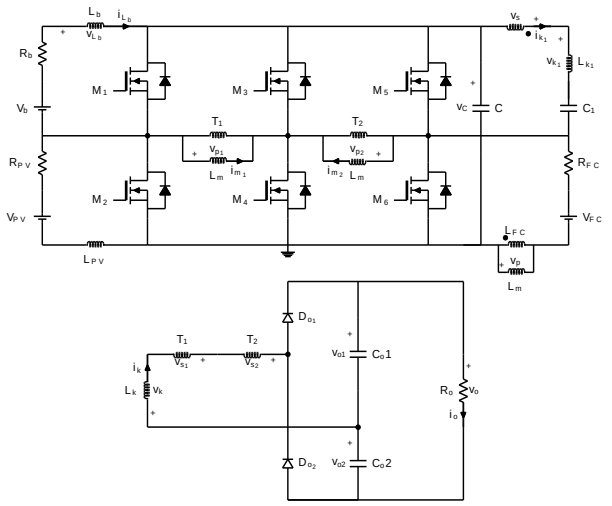

Fig. 2. Proposed converter in details

Interval 3 $[t_2, t_3]$: in this interval at first, the switches 1 and 5 is turned off. By considering the fact that the secondary currents of the transformers is referred to the primary side by the turn ratio factor of the transformers, hence in this interval, the capacitor of the drain sources for the switches 2 and 6 is started to discharge by using the energy of the magnetizing elements of the transformers and C_{DS} of the switches 1 and 5 is charged. Full discharging the C_{DS} of the switches 2 and 6, prepares these switches for soft switching in the beginning of the next interval.

Interval 4 $[t_3, t_d]$: at the starting point of this interval, the switches 2 and 6 are turned on and the voltage across the transformers will be zero. So, in this interval the energy is not transmitted to the load. The relation for L_k in this interval can be expressed as follows

$$L_k \frac{di_k}{dt} = -v_{o1} \quad (6)$$

In addition, the inductors L_{PV} and L_{m1} are charged and the inductor L_b discharges. Accordingly, the other equations in this interval can be written in the following.

$$L_{PV} \frac{di_{PV}}{dt} = V_{PV} \quad (7)$$

$$L_b \frac{di_b}{dt} = V_b - V_C \quad (8)$$

$$L_m \frac{di_m}{dt} = V_{FC} \quad (9)$$

$$L_{K1} \frac{di_{k1}}{dt} = n(V_{FC}) - V_{C1} \quad (10)$$

At the end of this interval, the diode D_{o1} current will be zero.

Interval 5 $[t_d, t_4]$: by removing the diode current in the beginning of this interval, the output load is only supplied through the output capacitors and both transformers are in freewheeling state. Since, no changes occur in the switches' states, the mathematical model for this interval can be expressed as follows:

$$L_k \frac{di_k}{dt} = 0 \quad (11)$$

$$L_{PV} \frac{di_{PV}}{dt} = V_{PV} - V_C \quad (12)$$

$$L_b \frac{di_b}{dt} = V_b \quad (13)$$

$$L_m \frac{di_m}{dt} = V_{FC} - V_C \quad (14)$$

$$L_{K1} \frac{di_{k1}}{dt} = n(V_{FC} - V_C) - V_{C1} \quad (15)$$

Interval 6 $[t_4, t_5]$: in this interval at first, the switch 4 is turned off. Hence in this interval, the capacitor of the drain source of the switch 3 is started to discharge by using the energy of the transformers magnetizing inductor and C_{DS} related to the switch 4 is charged. Full discharging the switch 3 will provide the soft switching condition for these switches in the beginning of the next interval.

Interval 7 $[t_5, t_6]$: the switch M_3 is turned on at the starting point of this interval. Therefore, the voltage across both transformer will be negative. This negative voltage is referred to the secondary side of the transformer. It causes the diode D_{o2} to be turned on. So, the expression for this interval will be as the following,

$$L_k \frac{di_k}{dt} = -2(n_1 + n_2)v_C + v_{o2} \quad (16)$$

Interval 8 $[t_6, t_7]$: in the beginning of this interval, the gate pulse of the switch 2 is cut off. So, by using the

magnetizing and leakage inductance energies, the capacitor of the drain source for the switch 2 is charged and the capacitor of the switch 1 is discharged and then its body diode is turned on. Therefore, at the end of this interval, the switch 1 is prepared to be turned on in the soft switching state.

Interval 9 $[t_7, t_8]$: when the switch 1 is turned on in zero voltage, the secondary voltage of the transformer 1 will be equal to zero. So, the total voltage across the equivalent leakage inductance is inversed and the diode D_{o2} is started to decrease with a low slope. In this interval, an equation for L_k would be as follows

$$L_k \frac{di_k}{dt} = -2(n_2)v_C + v_{o2} \tag{17}$$

Interval 10 $[t_8, t_9]$: In this interval, the switch 6 is turned off. So, by using the magnetizing and leakage inductance energies, the capacitor of the drain source for the switch 6 is charged and the capacitor of the switch 5 is discharged and then its body diode is turned on. Therefore, at the end of this interval, the switch 5 has been prepared to be turned on in soft switching state.

Interval 11 $[t_9, t_{11}]$: when the switch 5 is turned on, the secondary voltage of the transformer 2 is equal to zero and the diode D_{o2} current tends to move to zero by more rate. L_k current in this interval, would be as follows:

$$L_k \frac{di_k}{dt} = v_{o2} \tag{18}$$

3.2. The Converter Voltage Gain

In order to select the circuit elements, the output and the elements voltage are required. The volt-second law is applied to obtain the converter voltage gain for the equivalent leakage inductance of the transformers. Hence, a relation for the output voltage can be derived by regarding two following tips:

- Peak values for the currents of the diodes D_{o1} and D_{o2} can be determined by using the slope of the right side of the peak, or the slope of the left side of the peak.
- The diodes currents mean and the output currents are identical.

$$v_o = \underbrace{2(n_1+n_2)v_C\left(1-\frac{d}{d+\phi}\right)}_{v_{o1}} + \underbrace{2v_C[(n_1+n_2)(2\phi-1)+2n_1D_1+2n_2D_2]}_{v_{o2}} = \tag{19}$$

$$2(n_1+n_2)v_C\left(2\phi-\frac{d}{d+\phi}\right)+4v_C(n_1D_1+n_2D_2)$$

$$M=\frac{v_o}{v_C}=2(n_1+n_2)\left(2\phi-\frac{d}{d+\phi}\right)+4(n_1D_1+n_2D_2) \tag{20}$$

where, d in above expressions is defined by the fact that the diodes currents mean and the output current are the same, as the following

$$d=\frac{I_oT_S}{\phi v_C(n_1+n_2)} \tag{21}$$

It should be considered that the obtained voltage gain in this section, is the ratio of the output voltage to the low voltage DC link.

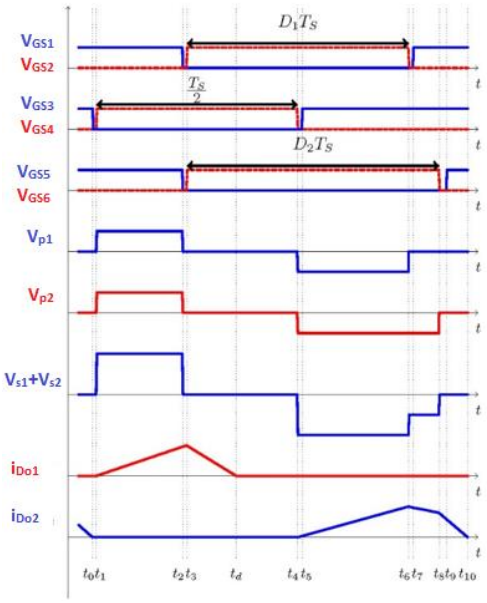

Fig. 3. Key waveforms

3.3. Power Management in the Converter

The power transmission between energy resources in the proposed converter is defined as follows: since the boost converters are used as an interface between the low voltage DC link and energy resources, the simplified equivalent circuit of the proposed converter can be decreased, as shown in Fig. 4 the parameters indicated on this figure are defined in table 1. Based on this figure, the resistance of the voltage resources determines the energy rate between various ports of the converter.

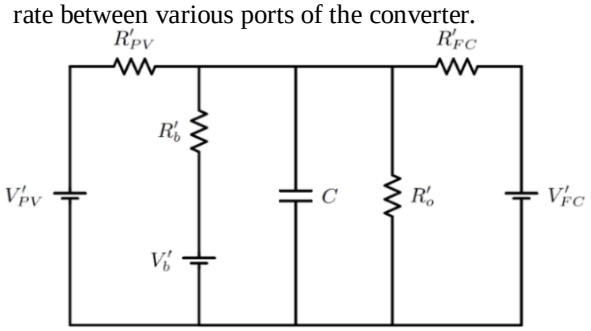

Fig. 4. Conceptual equivalent circuit for power management purposes.

A relation for the DC link voltage i.e. V_C, can be defined by using the circuit shown in Fig. 4. It is,

$$V_C=\frac{\frac{V'_{PV}}{R'_{PV}}+\frac{V'_b}{R'_b}+\frac{V'_{FC}}{R'_{FC}}}{\frac{1}{R'_{PV}}+\frac{1}{R'_b}+\frac{1}{R'_{FC}}+\frac{1}{R'_o}} \tag{22}$$

Now, the voltage source which receives the power, should have an equivalent voltage (which is indicated by superscript prime in Fig. 4) smaller than the DC link voltage i.e. V_C.

Table 1. Parameters used in Fig. 4.

V'_{PV}	V'_b	V'_{FC}	
$\frac{V_{PV}}{1-D_1}$	$\frac{V_b}{D_1}$	$\frac{V_{FC}}{1-D_2}$	
R'_{PV}	R'_b	R'_{FC}	R'_o
$\frac{R_{PV}}{(1-D_1)^2}$	$\frac{R_b}{D_1^2}$	$\frac{R_{FC}}{(1-D_2)^2}$	$\frac{R_o}{M^2}$

3.4. Efficiency Calculation

Sketching a cooling system is one of the major sections in power electronic circuits design. Subsequently, evaluating the converter gain, which is somehow evaluating losses of different parts, is involved in Design Consideration section. Using the method of element by element to calculate the losses, would be a conventional method to determine the efficiency of power electronic systems. In this method, upon specifying all of the elements losses of the converter, the system efficiency is determined by the well-known expression as follows

$$\eta = \frac{P_{out}}{P_{out}+P_{losses}} \quad (23)$$

The converter losses consist of three substantial parts; the switches, the diodes, and the magnetic losses, which will be explained later. The switches losses are devided into two parts: switching and conducting losses. Switching losses expression is given by

$$P_{sw} = \frac{1}{2}V_{DS_1}I_{D_1}f_s t_{on} + \frac{1}{2}V_{DS_2}I_{D_2}f_s t_{off} \quad (25)$$

The first term in the above equation is negligible in soft switching converters. The conducting losses, which are in concern with ON state resistance of the switch, are derived by $R_{on}I_D^2$. Resistive, reverse recovery current, and diode voltage dropping losses produce the diodes losses. Resistive losses is inconsequential due to low resistance of the diodes. In addition, reverse recovery current losses are not considered for the soft switching ZCS converters. So, there is just one expression for the diode losses, that is $V_F I_D^{DC}$. Magnetic losses of any magnetic elements such as inductors, transformers, etc. are also the summation of core and copper losses. Core losses have constant values for various load powers, that are obtained from $P_{fe} = K_c F^{\alpha} B_{max}^{\beta}$. Copper losses are also obtained from $R_w I_w^2$ by determining the winding resistance, where w stands for the winding. By looking at the preceding relations, it may be accomplished to evaluate the losses of different parts of the converter and its efficiency for a 1.5 kW prototype converter in four states of load powers, as represented in table 2.

Table 2. Efficiency calculation for different output load.

Output Power (Watt)		100	500	1000	1500
		Power Losses (Watt)			
Switches	Switching	9.03	11.01	13.37	24.75
	Conducting	0.5747	2.446	6.527	12.88
Magnetic	Constant	20.6345	20.6345	20.6345	20.6345
	Copper	0.8935	3.5135	9.389	20.01
Diodes		0.3925	1.9814	3.994	6.325
Total (Watt)		31.52	39.58	53.91	84.6
Efficiency (%)		76.03	92.66	94.88	94.84

An efficiency diagram for this converter from no load to full load is demonstrated in Fig. 5. This figure explains the converter efficiency in three modes of power transmission. In mode 1, the load power is provided through three input ports. In mode 2, the photovoltaic energy may be properly enough to provide the load entirely. In addition, the surplus energy generated by the photovoltaic, is storing in the battery. So, in mode 3, the load power is produced by the battery and the photovoltaic sources, simultaneously. To have a sense about the efficiency of the converter with respect to other recently proposed converter, the converter of [16] has been simulated and the efficiency has been derived which is shown in Fig. 5. According to the figure, the efficiency of the proposed converter is higher. The reason is that the converter in [16] has a lower voltage gain which results in higher current stress on the switches.

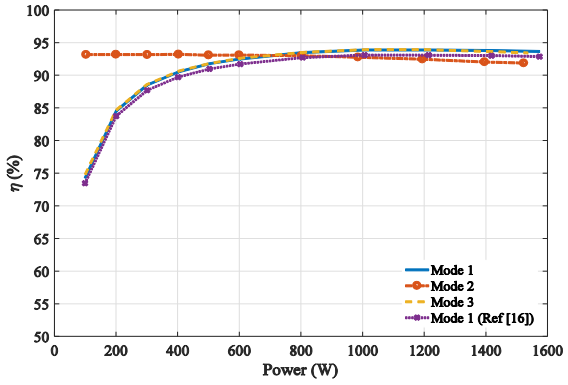

Fig. 5. Efficiency of the proposed converter.

4. EXPERIMENTAL RESULTS

A low power laboratory prototype was designed and tested experimentally, to validate the operation of the proposed converter. The parameters of the designed converter are as follows:

- PV port: 18-28V/6A
- FC port: 16-24V/7A
- Battery port: 24-32V/5A
- Output port: 200V/1A

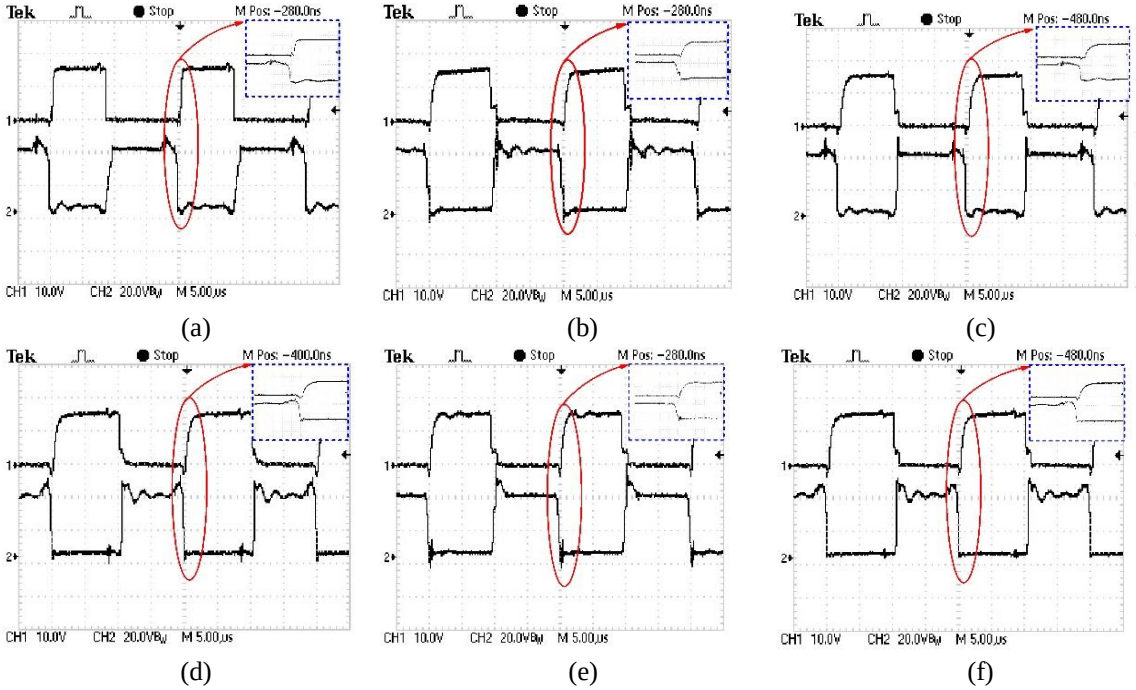

Fig. 6. Soft switching operation of switches. (a)-(f): $M_1 - M_6$

Table .3. Design parameters of proposed converter.

Spec.	Value
T_1, T_2	1:2-$L_m = 50\mu H$
L_{PV}, L_b	$50\mu H$
L_{FC}	2:1-$L_m = 80\mu H, L_k = 20\mu H$
D_1, D_2	MUR860
M_{1-6}	IXFH75N10

To show the ZCS operation of the proposed converter's diodes, the diode currents and the current of secondary of the transformers are shown in fig. 7. The currents D_{o1}, D_{o2}, and i_k are shown versus v_{s1} to show power the power transmission to the load in one switching cycle. Fig.7d shows switch S_2 current of the converter, Fig.7e illustrate the output voltage gain versus input current i_{FC}, and Fig.7f illustrates the primary current and voltage of transformer T_1. According to fig.7e it is obvious that very low ripple current flows through FC port which is one

The aim of this prototype is to show the key waveforms of the converter and soft switching operation.

Fig.6 illustrates the soft switching operation of the proposed converter. According to this figure all switches can operate in soft switching operation. The figure shows

The switching frequency is 50 kHz. Other specification of the converter are shown in table 3.

to view of the waveforms for clarity.

important feature of the proposed converter. Maximum efficiency of the converter was measured as 93.8% while the output load was supplied by all input ports. The experimental prototype of the proposed converter is shown in Fig. 8.

To show the controllability of the converter, a simulation has been done in the MATLAB/SIMULINK®. A 250W PV module is used in the simulation. In this simulation the Perturb and Observe (PandO) has been utilized to get the maximum possible power from the PV source. The simulation result is shown in Fig. 9 in which, at start of the simulation, the irradiation equal to 600W/m^2 is applied to the PV module. According to this figure, at the start of the simulation the PV module does not generate power and the total required power is provided by the battery. By producing power by PV, the MPPT algorithm result in generation of 150W. Accordingly, the battery power is reduced to 50W and the rest is supplied by the PV module.

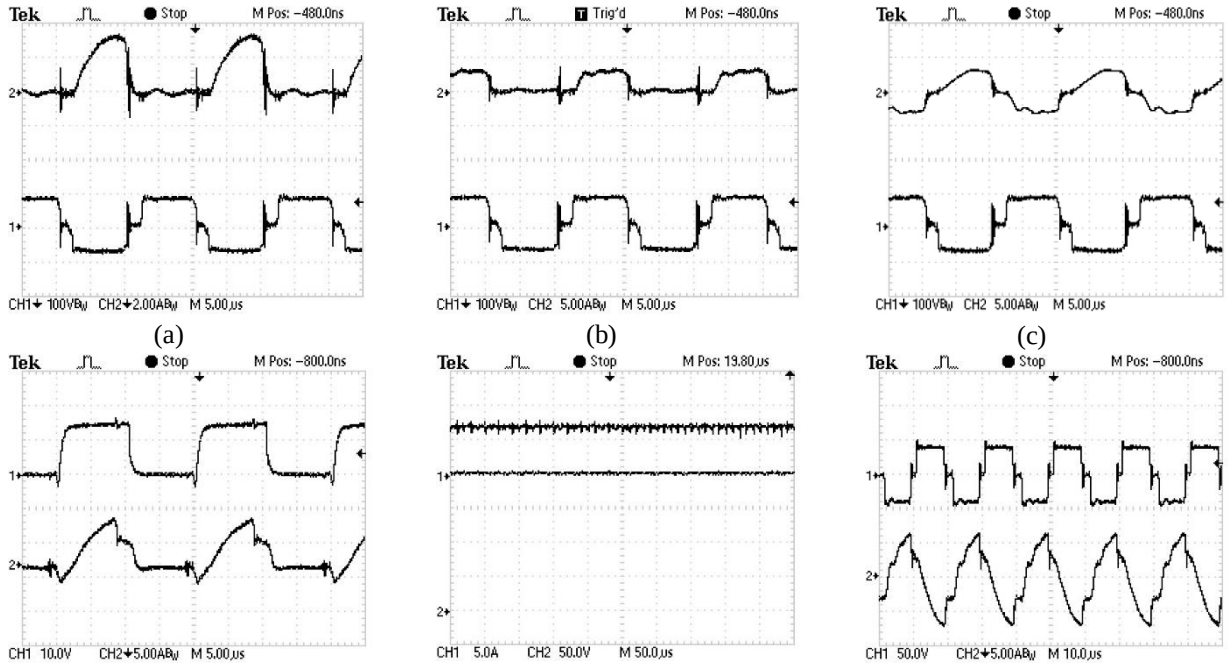

Fig. 6. (a), (b): D_{o1} and D_{o2} currents (top), transformer voltage(bottom) (c) i_k and voltage of secondary of transformers, (d) M_2: V_{gs} and I_D,(e) CH1: i_{FC}, CH2: v_o (f): V_p, i_p of transformer T_1.

Fig. 8. The experimental prototype of the proposed converter.

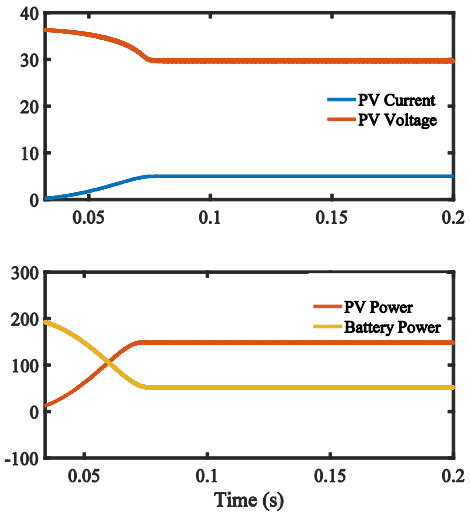

Fig. 9 . MPPT performance of the proposed converter

5. COMPARISON

This section deals with a comparison between the proposed converter and another multi input DC-DC converter. To have a fair comparison, the converter presented in [16] is selected. Both converters utilize bridge structures to transfer the power to high voltage side. Table 4 presents the main features of both converters. According to this table, the converters utilize the same resources such as switches or inductors. However, by splitting the power, and transfer using two transformers, higher voltage gain has been achieved in the proposed converter. Moreover, in the case that a switch leg does not work correctly, the proposed structure provides a second pass using 2 remaining switch legs and a transformer, to transfer the power to the high voltage DC-link. To achieve such features, although two transformer are used, but the size is smaller that the single transformer of the converter in [16].

Table 4. Performance comparison

Parameter	Ref. [16]	Proposed converter
NO. switches	6	6
NO. didoes	0	2
NO. inductors	3	3
NO. transformers	1 (big)	2 (small)
Ideal voltage gain	$\frac{n}{(1-D)}$	$\frac{4n}{1-D}$
Soft switching	Yes	Yes
Power Paths	1	2(more reliable)

6. CONCLUSION

This paper presented a multi-input high voltage gain converter to be used in hybrid supply systems for photovoltaic, fuel cell, and battery. The coupled inductor used in the proposed converter resulted in a ripple free input current for fuel cell, as it was validated in the experimental results. The zero voltage operation of the switches and zero-current switching of the diodes were illustrated in the operation of the prototype. These features leads the power supply system to be quiet from the EMI perspective. As it was mentioned in the paper, utilizing six switches result in two power path which increases the reliability of power supply system. Eventually the proposed converter is validated by a 200 Watt experimental prototype.

REFERENCES

[1] M. S. Manoharan, A. Ahmed, J.-W. Seo and J.-H. Park, "Power conditioning for a small-scale PV system with charge-balancing integrated micro-inverter," *J. Power Electron.*, vol. 15, no. 5, pp. 1318-1328, 2015.

[2] H. W. Ping, N. A. Rahim and J. Jamaludin, "New three-phase multilevel inverter with shared power switches," *J. Power Electron.*, vol. 13, no. 5, pp. 787-797, 2013.

[3] M. Moradzadeh, S. Hamkari E. Zamiri, and R. Barzegarkhoo, "Novel high step-up DC/DC converter structure using a coupled inductor with minimal voltage stress on the main switch," *J. Power Electron.*, vol. 16, no. 6, pp. 2005-2015, 2016.

[4] N. Mohan, W. Robbins and T. Undeland, "Power electronics: converters, applications, and design," 2003.

[5] R. W. Erickson and D. Maksimovic, *Fundam. Power Electron.*, Springer, 2001.

[6] C. Yaow-Ming, L. Yuan-Chuan and W. Feng-Yu, "Multi-input DC/DC converter based on the multiwinding transformer for renewable energy applications," *Ind. Appl. IEEE Trans.*, vol. 38, no. 4, pp. 1096-1104, 2002.

[7] L. Cao, K. H. Loo, Y. M. Lai, C. K. Tse and Y. Yang, "A multi-input bi-directional converter with decoupled power distribution control," *Proc.* 38th *Annu. Conf. IEEE Ind. Electron. Soc.*, 2012, pp. 3346-3351.

[8] M. M. Amin and O. A. Mohammed, "A novel grid-connected multi-input boost converter for HEVs: Design and implementation," Proc. *IEEE Int. Conf. Electr. Veh.*, 2012, pp. 1-7.

[9] Z. Rehman, "Multiport power electronics circuitry for integration of renewable energy sources in low power applications: a thesis presented in partial fulfilment of the requirements for the degree of Doctor of Philosophy in Electrical Engineering at Massey University, Palmerston North, New Zealand." *Massey University*, 2017.

[10] S. Xiaofeng, P. Guangming, Y. Shuai and C. Zhe, "A novel multi-port DC/DC converter with bi-directional storage unit," Proc. 7th *Int. Conf. Power Electron. Motion Control*, 2012, vol. 3, pp. 1771-1775.

[11] A. Khaligh, C. Jian and L. Young-Joo, "A multiple-input DC-DC converter topology," *IEEE Trans Power Electron.*, vol. 24, no. 3, pp. 862-868, 2009.

[12] H. Matsuo, T. Shigemizu, F. Kurokawa and N. Watanabe, "Characteristics of the multiple-input DC-DC converter," Proc. *IEEE* 24th *Annu. Power Electron. Spec. Conf.*, 1993, pp. 115-120.

[13] W. Hongfei, S. Kai, D. Shun and X. Yan, "Topology derivation of nonisolated three-port DC-DC converters from DIC and DOC," *IEEE Trans. Power Electron.*, vol. 28, no. 7, pp. 3297-3307, 2013.

[14] R. Jie, L. Fuxin, R. Xinbo, Y. Dongsheng, L. Yan and J. Ke, "Isolated multiple-input DC/DC converter using alternative pulsating source as building cells," Proc. *Int. Power Electron. Conf.*, 2010, pp. 1463-1470.

[15] Z. Qian, O. Abdel-Rahman and I. Batarseh, "An integrated four-port DC/DC converter for renewable energy applications," *IEEE Trans. Power Electron.*, vol. 25, no. 7, pp. 1877-1887, 2010.

[16] B. Mangu, S. Akshatha, D. Suryanarayana and B. G. Fernandes, "Grid-connected PV-wind-battery-based multi-input transformer-coupled bidirectional DC-DC converter for household applications," *IEEE J. Emerg. Sel. Top. Power Electron.*, vol. 4, no. 3, pp. 1086-1095, Sep. 2016.